Unoccupied states of individual silver clusters and chains on Ag(111)

A. Sperl, J. Kröger,* N. Néel, H. Jensen, and R. Berndt
Institut für Experimentelle und Angewandte Physik, Christian-Albrechts-Universität zu Kiel, D-24098 Kiel, Germany

A. Franke and E. Pehlke
Institut für Theoretische Physik und Astrophysik, Christian-Albrechts-Universität zu Kiel, D-24098 Kiel, Germany
(Received 18 September 2007; revised manuscript received 4 December 2007; published 20 February 2008)

Size-selected silver clusters on Ag(111) were fabricated with the tip of a scanning tunneling microscope. Unoccupied electron resonances give rise to image contrast and spectral features which shift toward the Fermi level with increasing cluster size. Linear assemblies exhibit higher resonance energies than equally sized compact assemblies. Density functional calculations reproduce the observed energies within 0.6 eV and enable an assignment of the resonances to hybridized atomic $5s$ and $5p_z$ orbitals with silver substrate states.

DOI: 10.1103/PhysRevB.77.085422 PACS number(s): 68.37.Ef, 68.47.De, 73.20.At, 73.22.−f

I. INTRODUCTION

Metal clusters at the nanometer scale which are supported by surfaces or thin films are currently of significant interest. Transport properties,[1] catalytic efficiency[2] and selectivity,[3] as well as magnetic response[4] depend strongly on the size of these assemblies. Moreover, understanding the influence of the substrate on the electronic structure of clusters[5] is important for new cluster-based materials with tailored optical, catalytic, or magnetic properties. To this end, clusters may be decoupled from a metal surface by introducing an oxide thin film between the substrate and the deposited clusters.[6–10]

The preparation of clusters with a given size on a surface is not an easy task. The approaches used so far include the deposition of size-selected clusters directly onto surfaces,[11] onto layers of noble gas atoms,[12,13] and the aggregation of clusters in buffer layers.[14] An alternative approach to controlling the size and shape of clusters on a surface is to use atom manipulation with the tip of a scanning tunneling microscope. This technique was applied in a variety of investigations, for instance, manganese, iron, and cobalt dimers on NiAl(110),[15] nickel dimers[16] and chromium trimers[17] on Au(111), copper chains on Cu(111),[18] and manganese monomers to tetramers on Ag(111).[19] Quantum confinement of electronic states to chains and islands was also revealed for homogeneous metallic systems.[18,20–25]

Here, we report on studies of electronic properties of silver clusters fabricated by single-atom manipulation on Ag(111) using the tip of a low-temperature scanning tunneling microscope. As key results, we obtain that unoccupied resonances exhibit energies whose actual values depend on the size and the shape of the adatom clusters. In particular, linear and monatomically wide chains exhibit higher resonance energies than their equally sized compact counterparts. Moreover, confinement of the unoccupied resonance states to the linear assemblies is found. The energies of unoccupied resonances of monomers, dimers, and a long silver chain are in agreement with density functional theory calculations.

II. EXPERIMENT

Measurements were performed with a custom-built scanning tunneling microscope operated in ultrahigh vacuum at a base pressure of 10^{-9} Pa and at 7 K. The Ag(111) surface and chemically etched tungsten tips were cleaned by argon ion bombardment and annealing. Individual silver atoms were deposited onto the sample surface by controlled tip-surface contacts as previously described in Ref. 26. Clusters with sizes ranging from one to eight atoms were fabricated by single-atom manipulation. For tunneling resistances of $\approx 10^5\ \Omega$, dragging of single silver atoms was feasible. Coalescence of adsorbed atoms (adatoms) to dimers up to octamers was accomplished by moving single adatoms close enough to the coalescence partner ($\approx$ one nearest-neighbor distance). We notice a propensity of silver adatoms to coalesce into compact assemblies rather than into linear clusters. For instance, adding an adatom to an already existing dimer in most cases resulted in a compact trimer rather than in a three-adatom chain. Silver chains containing more than 100 atoms were prepared by moving the tip toward the surface by 3–5 nm. Various surface dislocations were observed to result from this procedure. In particular, extraordinarily long and monatomically wide chains were found several hundreds of nanometers apart from the indentation area. Spectra of the differential conductance (dI/dV) were acquired by superimposing a sinusoidal voltage signal (root-mean-square amplitude of 1 mV and frequency of 10 kHz) onto the tunneling voltage and by measuring the current response with a lock-in amplifier. Prior to and in between spectroscopy of the clusters, the tip status was monitored by spectroscopy of the Ag(111) surface state band edge. Tips were prepared by controlled indentation into the substrate. Due to this treatment, we expect the tip apex to be covered with substrate material. All scanning tunneling microscopy (STM) images were acquired in the constant current mode, with the voltage applied to the sample.

III. THEORY

The total energy of the electronic ground state and the Kohn-Sham eigenenergies have been calculated for the silver monomer and dimer configurations on Ag(111) using the Vienna *ab initio* simulation package (VASP).[27–29] Moreover, the Ag chain on Ag(111) has been calculated using the total energy package FHI96MD.[30] Both program packages are based

on density functional theory with the generalized gradient approximation (GGA) (monomer and dimer: PW91;[31] chain: PBE[32]) applied to the exchange correlation functional. These GGAs are expected to yield comparable results. For the monomer and dimer configurations, the electron-ion interaction is treated within the framework of Bloechl's projector augmented wave (PAW) method.[33,34] For the calculation of the Ag chain, a Troullier-Martins pseudopotential has been generated with the FHI98PP (Ref. 35) program. The monomer and dimer configurations have been modeled in a slab geometry comprising 14 layers of silver and a (4×4) or (5×4) surface unit cell, respectively. For the chain configuration, the slab geometry consisted of 14 silver layers and a (9×1) surface unit cell. Perpendicular to the surface, the periodically repeated silver slabs are separated by a vacuum region of approximately 1.7 nm, which has been the subject of convergence tests and proved to be sufficient. In all calculations presented here, symmetric slabs were chosen such that the adsorption geometry is the same on both sides of the slab. The Kohn-Sham wave functions are expanded in a plane wave basis set, with a cutoff energy of 250 eV being sufficient in the case of the PAW potential. A larger cutoff energy of 544 eV had to be used for the norm conserving Troullier-Martins pseudopotential. The integrals over the Brillouin zone are approximated by sums over special k points[36] using meshes consisting of 16, 9, and 6 k points in the complete first Brillouin zone for the monomer, dimer, and chain, respectively. The local density of states (LDOS) has been calculated using the latter k point meshes in the case of the monomer and dimer. Additionally, to accurately sample the dispersion of the unoccupied state close to the lower one-dimensional band edge, a mesh of 144 special k points[36] in the first Brillouin zone has been used for the Ag chain. The Kohn-Sham wave functions at these additional k points have been calculated via so-called band structure runs, which are carried out at a frozen electron density from a previous self-consistent relaxation. The densities of states have been convoluted with a Lorentzian with a full width at half maximum of 150 meV. Convergence tests for the silver monomer using an eight layer slab show that upon increasing the cutoff energy to 300 eV, the calculated Kohn-Sham eigenenergies change by less than 15 meV. Increasing the number of k points for the dimer calculation to 16 leads to a change in the Kohn-Sham eigenenergies at $\bar{\Gamma}$ of less than 10 meV (in a test calculation for an eight layer slab).

Using the norm conserving pseudopotential and the PBE-GGA for exchange and correlation, the equilibrium lattice constant of silver is calculated to be 0.419 nm. The result is very similar (0.417 nm) when the PAW pseudopotential is used together with the PW91-GGA for exchange and correlation. These values are slightly larger than the experimental lattice constant of 0.409 nm, but the slight overestimate is consistent with other density functional calculations, e.g, for noble metals using GGA functionals.[37] The slabs were set up using the respective theoretical lattice constants. The silver atoms of the outermost three layers on both sides of the slab as well as the adatoms were allowed to relax without constraints until the residual forces per atom were smaller than 7×10^{-4} hartree/bohr. The remaining layers of the slab were kept fixed at their ideal bulk positions. For the calculation of the monomer, one silver adatom is relaxed above the face-centered cubic (fcc) hollow site on both sides of the slab, corresponding to a coverage of one adatom per 16 surface atoms. For the dimer calculation, two silver adatoms are relaxed above adjacent fcc hollow sites on both sides of the slab, corresponding to a coverage of one dimer per 20 surface atoms. The chain geometry consists of silver atoms adsorbed at next-neighbor fcc hollow sites in the direction of the chain.

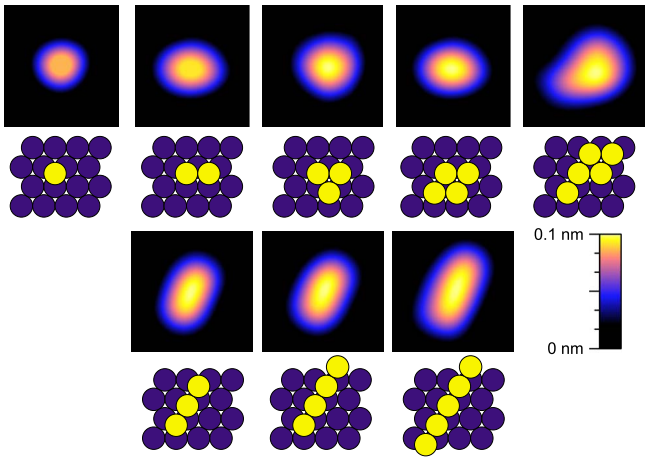

FIG. 1. (Color online) STM images of silver monomer, dimer, trimer, tetramer, and pentamer (from left to right) together with sketches of the proposed atomic arrangements (dark and bright circles depict substrate atoms and adsorbed atoms, respectively). Sample voltage and tunneling current were $V=100$ mV and $I=0.1$ nA. Image sizes: 2.1×2.1 nm^2 for $Ag_1,\ldots,Ag_5$ and 3×3 nm^2 for the linear tetramer and pentamer.

IV. RESULTS AND DISCUSSION

A. Compact and linear silver clusters: From monomer to octamer

Compact as well as linear assemblies were produced up to sizes of five and eight, respectively. STM images of single clusters are presented in Fig. 1 along with schematic models of their atomic arrangements. In these models, silver adatoms are placed at threefold coordinated fcc sites of the Ag(111) lattice. Table I compares apparent heights and full widths at half maximum (FWHMs) of linear assemblies with sizes ranging from a monomer to an octamer. Cross-sectional profiles of STM images were evaluated to this end. Per additional silver atom, the length of the chains increases by 0.28 nm on average, which is in good agreement with the nearest-neighbor distance of Ag(111). Starting from the trimer, the apparent height is 0.10 nm for all subsequent silver assemblies.

We notice that the silver dimer appears elongated in STM images (axes $\approx$1.28 nm and $\approx$1.06 nm). The orientation of the dimers is stable on the time scale of the experiment. These observations are in some contrast to previous results for Cu dimers on Cu(111),[38] where Cu_2 appeared nearly circular in STM images. This observation was attributed to in-

TABLE I. Apparent heights and FWHMs of silver clusters extracted from cross-sectional profiles of STM images. The FWHM refers to the longest lateral dimension of linear assemblies. All apparent heights and full widths at half maximum were measured at 0.1 V and 0.1 nA.

Cluster	Height (nm)	FWHM (nm)
Ag_1	0.06	1.1
Ag_2	0.08	1.3
Ag_3	0.10	1.6
Ag_4	0.10	1.7
Ag_5	0.10	2.1
Ag_6	0.10	2.3
Ag_7	0.10	2.7
Ag_8	0.10	3.0

tracell diffusion, i.e., the dimer moved within a cell of adjacent hexagonal close-packed and fcc sites centered around an on-top site.

Next we focus on unoccupied electronic states of the silver assemblies. Figure 2 shows a series of normalized dI/dV spectra acquired with the tip positioned above the center of compact clusters. The tunneling gap for spectroscopy was

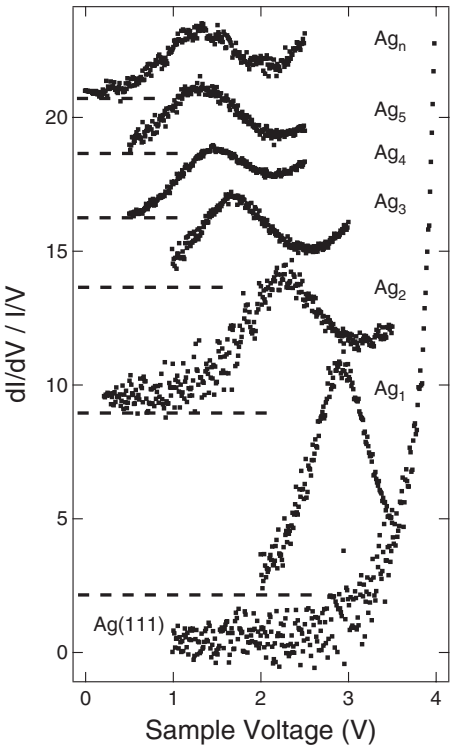

FIG. 2. Normalized spectra of dI/dV acquired on clean Ag(111), monomers (Ag_1), dimers (Ag_2), trimers (Ag_3), tetramers (Ag_4), and pentamers (Ag_5). A compact silver assembly (Ag_n) with probably $n \approx 10$ was also analyzed. The tunneling gap for the spectra was set at 1 nA and 3.5 V (Ag_1 and Ag_2), 3.0 V (Ag_3), and 2.5 V (Ag_4, Ag_5, and Ag_n). Spectra of Ag_n ($n \geq 1$) are vertically offset for clarity. The dashed lines indicate the respective zero of the spectra.

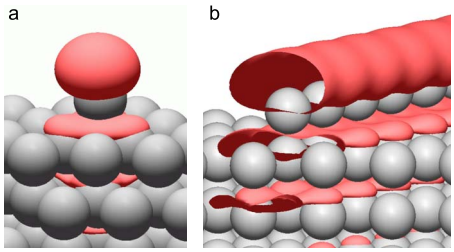

FIG. 3. (Color online) Contour plots of the absolute square of the Kohn-Sham wave function at $\bar{\Gamma}$ for (a) the silver monomer and (b) the silver chain. The corresponding Kohn-Sham eigenenergies relative to the Fermi level are 2.66 eV for the Ag monomer and 1.37 eV for the Ag chain.

stabilized at 1 nA and 3.5 V for Ag_1, Ag_2, 3.0 V for Ag_3, and 2.5 V for Ag_4, Ag_5, and Ag_n. Due to different tip-cluster distances for the various spectra, we normalized the dI/dV data sets by the conductance I/V according to Refs. 39–41. The spectrum of clean Ag(111) is featureless up to ≈3.5 eV. A steady increase at higher sample voltages is attributed to field emission resonances.[42,43] The spectrum of the Ag adatom exhibits a pronounced peak slightly below 3 eV. Spectra from the vicinity of and above the single atom revealed that spatial extension of the monomer resonance is comparable to the size of the atom in STM images. These results suggest that the silver monomer exhibits a quasiatomic resonance. This interpretation is in accordance with observations for single Au atoms on NiAl(110) (Ref. 1) and for Pd monomers on Al_2O_3 layers.[44] Thus, the enhanced normalized differential conductance can be attributed to resonant tunneling into an empty state of the Ag atom. Indeed, our calculations reveal that this state is of sp character arising from the hybridizaton of atomic Ag $5p_z$ orbitals with $5s$ admixtures localized at the adsorbate and silver substrate states. A typical wave function is shown in Fig. 3(a).

Spectra acquired on compact and linear clusters containing a higher number of atoms likewise exhibit a peak whose energy shifts to lower values with increasing cluster size.[45] Figure 4 summarizes the resonance energies for compact (triangles) and linear (circles) silver clusters of different sizes. The spectra were acquired atop the center of the assemblies. The resonance energies for compact clusters are lower than those for their equally sized linear counterparts. From Fig. 4, we further infer that for both cluster types, the change of the resonance energy becomes less pronounced with increasing cluster size. For instance, the energy of the compact pentamer resonance is at ≈1.5 eV, which already comes close to a compact assembly denoted Ag_n ($n \approx 10$) in Fig. 2. Lagoute *et al.*[21] investigated triangular Cu islands containing up to 15 atoms on Cu(111) and found an evolution of quasiatomic resonances to the two-dimensional Shockley-type surface state. In our case, the resonance energies of linear clusters clearly exceed the Ag(111) surface state energy (−70 meV) in the limit of large cluster sizes and are found to approach an asymptotic value of approximately 1.5 eV. This resonance energy is observed for a very long silver chain, which will be discussed in the following section. The situation for compact clusters is different. Our experimental data were measured

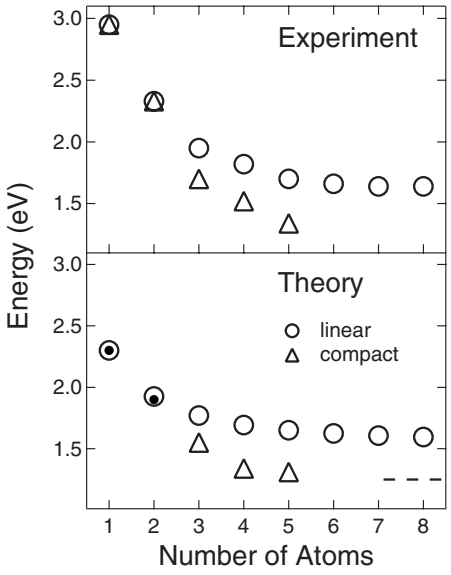

FIG. 4. Experimentally determined and calculated energies of unoccupied resonances as a function of cluster size. Resonance energies for compact (triangles) and linear (circles) assemblies are presented. Error margins for experimental energies ($\approx \pm 0.05$ eV) are the standard deviation resulting from a statistical analysis of spectra of a variety of clusters. Theoretical values calculated within a tight-binding model described in the text (open circles and triangles) are compared to *ab initio* Kohn-Sham eigenenergies (filled circles). The dashed line denotes the lower band edge of the dispersion of the chain states as obtained from density functional calculations. For each geometry, the lowest tight-binding eigenenergy is given. The island configurations refer to those displayed in Fig. 1. The compact islands enfold the trimer, the tetramer, and the pentamer.

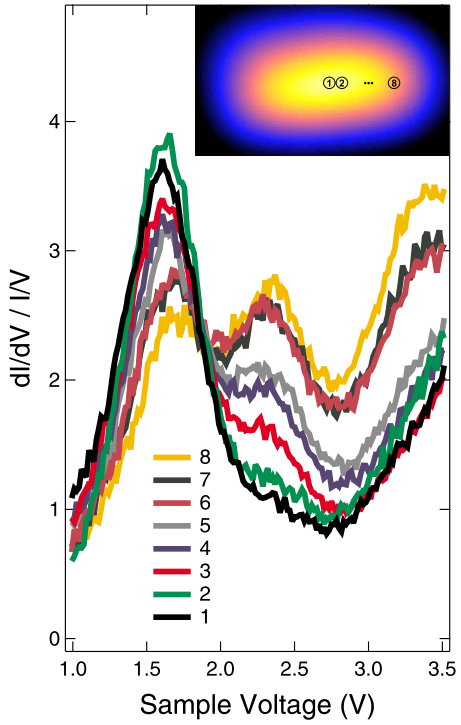

FIG. 5. (Color online) dI/dV spectra acquired at indicated (1,2,…,8) positions of a linear pentamer. Inset: STM image of linear pentamer showing the positions at which spectra were taken. The tunneling gap was set at 1 nA and 3.5 V.

on very small clusters and, we believe, it is not appropriate to extrapolate it to infinite cluster size. However, a close inspection of the density functional theory (DFT) results for the Kohn-Sham wave function of the Ag(111) surface state reveals its dominant p_z character similar to the resonance displayed in Fig. 3. This finding is complemented by the Ag $5p_z$ projected density of states at the Ag(111) surface which resembles a step function at the onset of the surface state. Our tight-binding interpolation is consistent with a convergence of the lowest-energy cluster eigenstate toward the lower band edge of the surface state with increasing size of the compact clusters. Thus, our interpretation is consistent with the findings of Lagoute *et al.* for the Cu(111) surface state in Ref. 21.

B. Monatomically wide silver chains

Here, we focus on electronic properties of monatomically wide silver chains. Figure 5 shows spatially resolved dI/dV spectra acquired at different sites on a linear pentamer (see inset of Fig. 5). The dI/dV spectrum taken atop the center of the assembly exhibits a single peak at $\approx$1.6 eV (to be compared also with Fig. 4). By performing spatially resolved spectroscopy along the linear cluster (spectra 2–8), a gradual trade of spectral weight from the resonance peak at $\approx$1.6 eV to an additional peak at $\approx$2.3 eV is observed. Moreover, compared to the resonance energy of $\approx$1.6 eV observed atop the middle of the chain, at its ends this energy has shifted up to $\approx$1.7 eV. By analyzing the dependence of the first and second peaks on the length of the chains, we found (not shown) that these peaks may be well described within a simple particle-in-a-box model. Similar confinement effects for unoccupied resonances were observed for Au chains on NiAl(110) (Ref. 1) and for Cu chains on Cu(111).[18]

How does the confinement evolve for chains containing a very large number of atoms? Starting from the linear octamer, it became difficult to resolve confinement-related peaks in dI/dV spectra, which may be related to overlap of neighboring peaks. Nevertheless, confinement was evidenced by localization of density of states at the ends of a very long chain, to be discussed next. The length of the chain is $\approx$45 nm and follows a close-packed direction of the hosting Ag(111) lattice. Consequently, the number of silver atoms is approximately 160. Figure 6 shows a normalized dI/dV spectrum of the resonance in the middle of the chain. We extract an energy of $\approx$1.5 eV for the resonance position. Our DFT calculations reproduce the energy of the peak in the case of an infinitely long chain [see an illustration of the wave function in Fig. 3(b) and compare Figs. 6 and 8].

In addition to the unoccupied resonance, STM images and spatial maps of dI/dV acquired at different voltages evidence confinement of the resonance within the chain. In Fig. 7(a), spatially resolved dI/dV data acquired along the chain at the indicated voltages are presented. At voltages exceeding 1.6 V, the differential conductance increases toward the ends

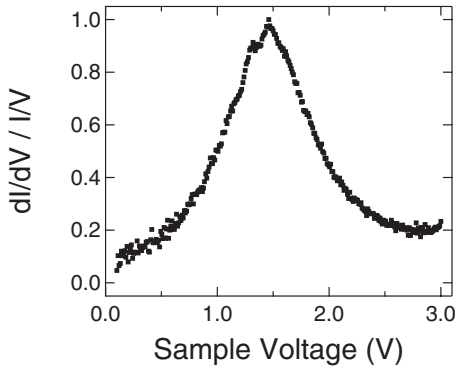

FIG. 6. Normalized spectrum of dI/dV at the center of an ≈45 nm long and monatomically wide silver chain. The tunneling gap was set at 0.6 nA and 3 V.

of the chain. Figures 7(b) and 7(c) show the evolution of the apparent height and the width (FWHM) of the chain (taken close to the middle of the chain) as a function of the applied voltage. A monotonous increase is observed for the apparent height as well as for the FWHM. At sample voltages between ≈1.5 and ≈1.7 V, height and width increase more rapidly than at other voltages. We attribute these observations to tunneling into the chain resonance.

C. Theoretical results

To compare experimental resonance energies with calculated results, we evaluated the LDOS at a position of ≈0.25 nm atop the adsorbed Ag atom for the monomer and the chain. For the dimer configuration, the LDOS was computed at approximately the same height atop the center of the dimer. The results are presented in Fig. 8. A similar LDOS for Cu chains on Cu(111) has been calculated by Stepanyuk *et al.*[46]

In case of the monomer, a resonance predominantly derived from Ag sp_z orbitals occurs at ≈2.3 eV above the Fermi energy [see Fig. 3(a)]. In case of the silver dimer, with Ag atoms occupying neighboring fcc sites, this resonance splits into a p_z bonding resonance at ≈1.9 eV and a p_z antibonding resonance.[47] The LDOS of the Ag chain is characterized by a one-dimensional band formed from an uncoccupied p_z-like resonance as shown in Fig. 3(b). The lower band edge of this one-dimensional band is located at ≈1.3 eV above the Fermi energy E_F (as derived from the electronic eigenenergies at $\bar{\Gamma}$). A peak arises at around 1.5–1.6 eV. No upper band edge of the one-dimensional band was observed for energies below the work function of silver. Table II summarizes experimental and calculated resonance energies. Owing to the agreement between experiment and theory, we interpret peaks in the dI/dV spectra as the signature of sp_z- or p_z-like Ag adsorbate resonances and their electronic interaction with silver substrate states.

We did not perform *ab initio* calculations for silver clusters of sizes larger than two atoms due to the large computational costs arising from the increasing size of the surface unit cell. However, we provide estimates for the electronic eigenenergies of larger clusters by means of a simple tight-

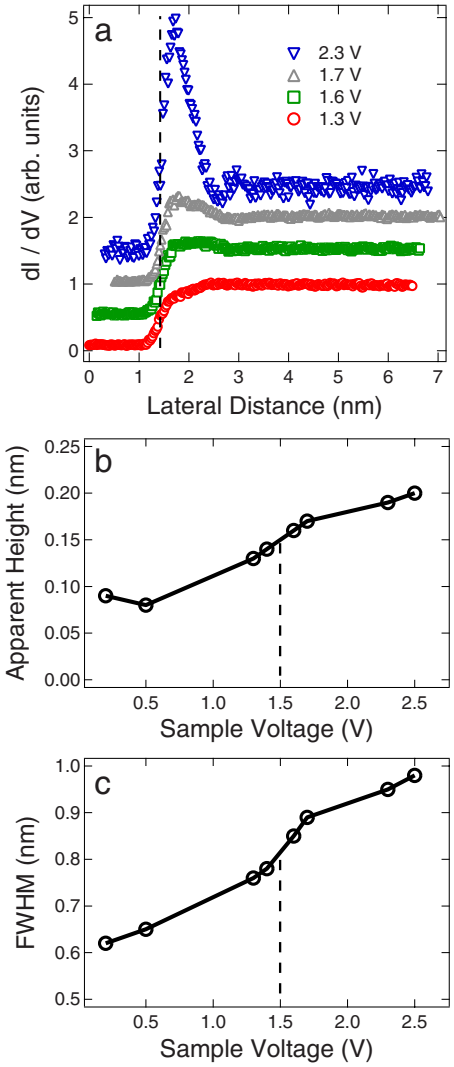

FIG. 7. (Color online) (a) Cross-sectional profiles in a map of dI/dV taken at the indicated voltages along the middle axis of the chain showing the increase of the signal at the end of the chain at a lateral displacement of ≈1.5 nm. The profiles acquired at voltages ⩾1.6 V are vertically offset for clarity. (b) Apparent height of the chain as a function of the applied voltage. (c) Like (b) for the full width at half maximum of the chain. Dashed lines in (b) and (c) indicate the chain resonance energy. Apparent heights and widths were taken close to the middle of the chain.

binding model.[21] The purpose of this estimate is to explain the energy shifts observed by tunneling spectroscopy semiquantitatively. In our tight-binding approach, the substrate is not considered explicitly, i.e., the islands are represented by freestanding two-dimensional clusters. We include one Ag sp_z orbital per atom. There are only two free tight-binding parameters: the orbital energy ε_0 and the next-neighbor transfer matrix element t, which accounts for the direct interaction between nearest-neighbor Ag atoms and, implicitly, part of the interaction via the Ag substrate. All further interactions with respect to more distant atoms are neglected, as is the variation of the crystal-field energy shift of the orbital energy for different geometrical environments. As usual, orbital overlaps are not accounted for explicitly.

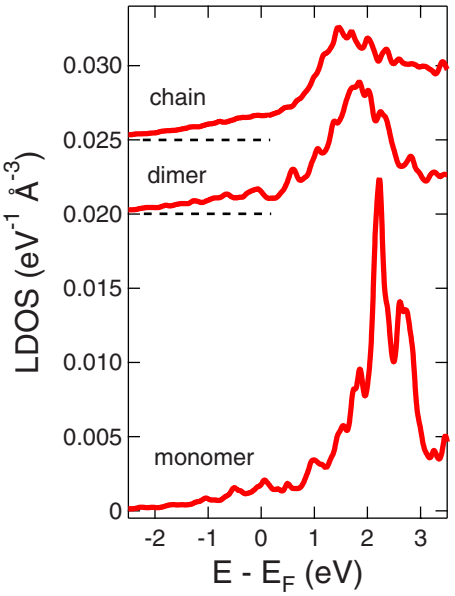

FIG. 8. (Color online) Calculated LDOS for a silver monomer (bottom), a silver dimer (middle), and an infinitely long silver chain (top) on Ag(111). Resonance energies inferred from these calculations are 2.3 eV, 1.9 eV, and 1.5–1.6 eV, respectively. The LDOS has been computed atop a silver adatom in the case of the monomer and the chain, and atop the center of the silver dimer. The dimer and chain LDOS were shifted vertically, with dashed lines indicating the respective zero LDOS.

The tight-binding parameters are consistently derived from our DFT results, i.e., the resonance energy of the monomer $\varepsilon_0=2.3$ eV (experimental value 2.9 eV) and the binding energy of the Ag(111) surface state at $\bar{\Gamma}$, $\varepsilon_0+6t=+0.05$ eV (experimental value ≈ -0.07 eV,[48] which is in agreement with earlier work),[49,50] are reproduced by the tight-binding model. The quality of the tight-binding results can be estimated from comparison with the DFT Kohn-Sham eigenenergies of the dimer and the chain shown in Fig. 4(b). The lowest-energy eigenvalue is given for each configuration. For further evaluation of the quality of the tight-binding model, we notice that for the effective mass m^* of the surface state, we obtain $0.8m_e$ (m_e is the free electron mass) from tight-binding calculations to be compared with a DFT value of $0.39m_e$ and an experimental value of $(0.42\pm0.02)m_e$ obtained by scanning tunneling spectroscopy.[48] The effective mass of the sp_z resonance at the one-dimensional Ag chain is $1.2m_e$ in our tight-binding approach to be compared with a value of about $0.6m_e$ derived from the dispersion of the Kohn-Sham eigenenergies close to $\bar{\Gamma}$. Most probably, the overestimate of the effective mass by a factor of 2 in both cases may partially be due to the fact that no parameter describing the crystal-field energy shift is included in the tight-binding Hamiltonion operator, giving rise to an inaccurate value of the transfer parameter.

TABLE II. Comparison of experimental (expt) and calculated (calc) energies (E) of unoccupied resonances.

Cluster	E^{expt} (eV)	E^{calc} (eV)
Monomer	2.9	2.3
Dimer	2.3	1.9
Chain	1.5	1.5–1.6

Nevertheless, the simple tight-binding approach provides all qualitative trends for the cluster eigenenergies [see Fig. 4(b)]. Compact clusters have lower eigenenergies than equally sized linear assemblies, and the trimer exhibits a lowest electronic eigenenergy which is close to the lower band edge of the infinite chain.

V. SUMMARY

Size-selected silver clusters were fabricated by tip-assisted single-atom manipulation on Ag(111). Unoccupied electronic resonances exhibit energies which are characteristic of the size and shape of the silver assemblies. In particular, the resonances of linear clusters have higher energies than the resonances of equally sized compact clusters. For both types of clusters, the resonance energy shifts toward the Fermi energy with increasing cluster size. Similar to the findings in Ref. 21, these observations are in qualitative agreement with a tight-binding model of the clusters. Calculations based on density functional theory model the energies of monomers, dimers, and monatomically wide infinitely long chains. The resonances are of *sp* character and arise from Ag $5p_z$ orbitals (with $5s$ admixtures) which are localized at the adsorbate atom and hybridize with silver substrate states.

ACKNOWLEDGMENT

Funding of this work by the Deutsche Forschungsgemeinschaft through SPP 1153 is gratefully acknowledged.

*kroeger@physik.uni-kiel.de

[1] N. Nilius, T. M. Wallis, and W. Ho, Science **297**, 1853 (2002).
[2] S. Abbet, A. Sanchez, U. Heiz, W.-D. Schneider, A. M. Ferrari, G. Pacchioni, and N. Rösch, J. Am. Chem. Soc. **122**, 3453 (2000).
[3] S. Abbet, A. Sanchez, U. Heiz, and W.-D. Schneider, J. Catal. **198**, 122 (2001).
[4] J. Bansmann, S. H. Baker, C. Binns, J. A. Blackman, J.-P. Bucher, J. Dorantes-Dávila, V. Dupuis, L. Favre, D. Kechrakos, A. Kleibert, K.-H. Meiwes-Broer, G. M. Pastor, A. Perez, O. Toulemonde, K. N. Trohidou, J. Touaillon, and Y. Xie, Surf. Sci. Rep. **56**, 189 (2005).
[5] A. S. Wörz, K. Judai, S. Abbet, J.-M. Antonietti, U. Heiz, A. Del Vitto, L. Giordano, and G. Pacchioni, Chem. Phys. Lett. **399**, 2666 (2004).
[6] R. M. Jaeger, H. Kuhlenbeck, H.-J. Freund, M. Wuttig, W. Hoffmann, R. Franchy, and H. Ibach, Surf. Sci. **259**, 235 (1991).
[7] U. Bardi, A. Atrei, and G. Rovida, Surf. Sci. **268**, 87 (1992).

[8] C. Becker, J. Kandler, H. Raaf, R. Linke, T. Pelster, M. Dräger, M. Tanemura, and K. Wandelt, J. Vac. Sci. Technol. A **16**, 1000 (1998).
[9] M. Bäumer and H.-J. Freund, Prog. Surf. Sci. **61**, 127 (1999).
[10] K. Hojrup Hansen, T. Worren, E. Lægsgaard, F. Besenbacher, and I. Stensgaard, Surf. Sci. **475**, 96 (2001).
[11] Y. Kuk, M. F. Jarrold, P. J. Silverman, J. E. Bower, and W. L. Brown, Phys. Rev. B **39**, 11168 (1989).
[12] K. Bromann, C. Félix, H. Brune, W. Harbich, R. Monot, J. Buttet, and K. Kern, Science **274**, 956 (1996).
[13] K.-H. Meiwes-Broer, *Metal Clusters at Surfaces*, Springer Series in Cluster Physics (Springer, Berlin, 2000).
[14] L. Huang, S. J. Chey, and J. H. Weaver, Phys. Rev. Lett. **80**, 4095 (1998).
[15] H. J. Lee, W. Ho, and M. Persson, Phys. Rev. Lett. **92**, 186802 (2004).
[16] V. Madhavan, T. Jamneala, K. Nagaoka, W. Chen, J.-L. Li, S. G. Louie, and M. F. Crommie, Phys. Rev. B **66**, 212411 (2002).
[17] T. Jamneala, V. Madhavan, and M. F. Crommie, Phys. Rev. Lett. **87**, 256804 (2001).
[18] S. Fölsch, P. Hyldgaard, R. Koch, and K. H. Ploog, Phys. Rev. Lett. **92**, 056803 (2004).
[19] J. Kliewer, R. Berndt, J. Minár, and H. Ebert, Appl. Phys. A: Mater. Sci. Process. **82**, 63 (2006).
[20] J. Li, W.-D. Schneider, R. Berndt, and S. Crampin, Phys. Rev. Lett. **80**, 3332 (1998).
[21] J. Lagoute, X. Liu, and S. Fölsch, Phys. Rev. Lett. **95**, 136801 (2005).
[22] H. Jensen, J. Kröger, R. Berndt, and S. Crampin, Phys. Rev. B **71**, 155417 (2005).
[23] S. Crampin, H. Jensen, J. Kröger, L. Limot, and R. Berndt, Phys. Rev. B **72**, 035443 (2005).
[24] J. Kröger, L. Limot, H. Jensen, R. Berndt, S. Crampin, and E. Pehlke, Prog. Surf. Sci. **80**, 26 (2005).
[25] J. Kröger, M. Becker, H. Jensen, Th. von Hofe, N. Néel, L. Limot, R. Berndt, S. Crampin, E. Pehlke, C. Corriol, V. M. Silkin, D. Sánchez-Portal, A. Arnau, E. V. Chulkov, and P. M. Echenique, Prog. Surf. Sci. **82**, 293 (2007).
[26] L. Limot, J. Kröger, R. Berndt, A. Garcia-Lekue, and W. A. Hofer, Phys. Rev. Lett. **94**, 126102 (2005).
[27] G. Kresse and J. Hafner, Pramana, J. Phys. **47**, 558 (1993).
[28] G. Kresse and J. Hafner, Comput. Mater. Sci. **6**, 15 (1996).
[29] G. Kresse and J. Furthmuller, Phys. Rev. B **54**, 11169 (1996).
[30] M. Bockstedte, A. Kley, J. Neugebauer, and M. Scheffler, Comput. Phys. Commun. **107**, 187 (1997).
[31] J. P. Perdew, J. A. Chevary, S. H. Vosko, K. A. Jackson, M. R. Pederson, D. J. Singh, and C. Fiolhais, Phys. Rev. B **46**, 6671 (1992).
[32] J. P. Perdew, K. Burke, and M. Ernzerhof, Phys. Rev. Lett. **77**, 3865 (1996).
[33] P. E. Blöchl, Phys. Rev. B **50**, 17953 (1994).
[34] G. Kresse and D. Joubert, Phys. Rev. B **59**, 1758 (1999).
[35] M. Fuchs and M. Scheffler, Comput. Phys. Commun. **116**, 1 (1999).
[36] H. J. Monkorst and J. D. Pack, Phys. Rev. B **13**, 5188 (1976).
[37] M. Fuchs, M. Bockstedte, E. Pehlke, and M. Scheffler, Phys. Rev. B **57**, 2134 (1998).
[38] J. Repp, G. Meyer, K.-H. Rieder, and P. Hyldgaard, Phys. Rev. Lett. **91**, 206102 (2003).
[39] R. M. Feenstra, J. A. Stroscio, and A. P. Fein, Surf. Sci. **181**, 295 (1987).
[40] N. D. Lang, Phys. Rev. B **34**, R5947 (1986).
[41] V. A. Ukraintsev, Phys. Rev. B **53**, 11176 (1996).
[42] R. S. Becker, J. A. Golovchenko, and B. S. Swartzentruber, Phys. Rev. Lett. **55**, 987 (1985).
[43] G. Binnig, K. H. Frank, H. Fuchs, N. Garcia, B. Reihl, H. Rohrer, F. Salvan, and A. R. Williams, Phys. Rev. Lett. **55**, 991 (1985).
[44] N. Nilius, T. M. Wallis, and W. Ho, Phys. Rev. Lett. **90**, 046808 (2003).
[45] The rapid rise of dI/dV due to the first field emission resonance (also referred to as "modified image state") dominates the spectra at higher voltages.
[46] V. S. Stepanyuk, A. N. Klavsyuk, L. Niebergall, and P. Bruno, Phys. Rev. B **72**, 153407 (2005).
[47] A. Sperl, J. Kröger, H. Jensen, R. Berndt, A. Franke, and E. Pehlke (unpublished).
[48] J. Li, W.-D. Schneider, and R. Berndt, Phys. Rev. B **56**, 7656 (1997).
[49] S. D. Kevan and R. H. Gaylord, Phys. Rev. B **36**, 5809 (1987).
[50] R. Paniago, R. Matzdorf, G. Meister, and A. Goldmann, Surf. Sci. **331-333**, 1233 (1995).